Steady-state solutions for subsurface chlorophyll maximum in stratified water columns with a bell-shape vertical profile of chlorophyll

X. Gong, J. Shi, H. W. Gao, X. H. Yao

Key Laboratory of Marine Environment and Ecology (Ministry of Education of China), Ocean University of China, Qingdao 266100, China

Correspondence to: H. W. Gao (hwgao@ouc.edu.cn)

Abstract:

A bell-shape vertical profile of chlorophyll a (Chl a) concentration, conventionally referred to as Subsurface Chlorophyll Maximum (SCM) phenomenon, has frequently been observed in stratified oceans and lakes. This profile is assumed to be a general Gaussian distribution in this study. By substituting the general Gaussian function into ecosystem dynamical equations, the steady-state solutions for SCM characteristics (i.e., SCM layer depth, thickness, and intensity) in various scenarios are derived. These solutions indicate that: 1) The maximum concentration of Chl a occurs at or below the depth of maximum growth rates of phytoplankton located at the transition from nutrient limitation to light limitation, and the depth of SCM layer deepens logarithmically with an increase in surface light intensity; 2) Thickness and intensity of the SCM are mainly affected by nutrient supply, but independent of surface light intensity; 3) The intensity of SCM layer is proportional to the diffusive flux of nutrients from below, getting stronger as a result of this layer being shrunk by a higher light attenuation coefficient or a larger sinking velocity of phytoplankton. In addition, the limitation and potential application of the analytical solutions are also presented.

1 Introduction

Vertical profiles of chlorophyll a (Chl a) concentration in lakes, coastal seas and open oceans are highly variable. However, a bell-shape vertical profile of Chl a, conventionally referred to as Subsurface Chlorophyll Maximum (SCM) phenomenon, has been frequently observed in stratified water columns, e.g., it occurs through the whole year in tropical and subtropical oceans while it exists only during summer in temperate and high latitude oceanic zones. The subsurface biomass maxima (SBMs) are also common in stratified water columns. The chlorophyll-to-biomass ratio generally increases with depth in the euphotic zone. Thus, SCMs may not necessarily represent SBMs (Cullen, 1982; Fennel and Boss, 2003) and are usually deeper than SBMs (Fennel and Boss, 2003; Hodges and Rudnick, 2004). However, both the subsurface maxima in chlorophyll and biomass are usually formed in certain regions of the water column where two opposing resource (light and nutrient) gradients combined with turbulent mixing is amenable for survival of phytoplankton. Thus, SCMs are approximately equal to SBMs in many studies (Klausmeier and Litchman, 2001; Sharples et al., 2001; Huisman et al., 2006; Raybov et al., 2010). Fennel and Boss (2003) reported that the photoacclimation of phytoplankton can be another important reason for forming a SCM in oligotrophic waters.

The SCM phenomenon can be characterized by the thickness, depth, and intensity of SCM layer (SCML) (Beckmann and Hense, 2007). On-site observations (Platt et al., 1988; Sharples et al., 2001; Dekshenieks et al., 2001; Mellard et al., 2011) showed that the SCML occurred relatively shallow (1-50 m) and was thin (several centimeters to a few meters) in lakes and coastal seas, but the concentration of Chl a was high (1-100 mg/m^3). In open oceans, the SCML was deeper (80-130 m) and thicker (tens of meters) while the concentration of Chl a was relatively low (<1 mg/m^3) (Anderson, 1969; Platt et al., 1988).

SCMs have attracted much attention because of the significant contribution of SCML to the total biomass and primary production in the whole water column (Cullen and Eppley, 1981; Weston et al., 2005; Siswanto et al., 2005; Hanson et al., 2007; Sullivan et al., 2010). Pérez et al. (2006) showed that 65-75% of the total Chl a in a water column of the Atlantic subtropical gyres was presented in SCML and the layer thickness was approximately 50 m. Weston et al. (2005) reported that the SCML

57 accounted for 58% of the water column primary production in the central North Sea,
58 although the layer thickness was less than 5 m. Sullivan et al. (2010) found that the
59 fraction of Chl a in the SCML (thickness <3 m) out of the total water column ranged
60 from 33% to 47% in the Monterey Bay.

61 Many numerical studies have been conducted to link the thickness, depth and
62 intensity of the SCML to various environmental parameters (Jamart et al., 1979;
63 Varela et al., 1994; Klausmeier and Litchman, 2001; Hodges and Rudnick, 2004;
64 Huisman et al., 2006; Beckmann and Hense, 2007). The thickness of the SCML
65 mainly depends on the degree of vertical mixing in lakes (Klausmeier and Litchman,
66 2001). In oligotrophic oceans, light attenuation coefficient is the key factor in
67 determining the SCML depth (Varela et al., 1994; Hodges and Rudnick, 2004;
68 Beckmann and Hense, 2007) and the intensity of the SCML depends strongly on
69 sinking velocity of phytoplankton and/or detritus and vertical diffusivity rather than
70 growth rate of phytoplankton (Hodges and Rudnick, 2004; Beckmann and Hense,
71 2007). However, the thickness, depth and intensity of SCML are very sensitive to
72 variations of environmental parameters. Therefore, the relationships obtained from a
73 particular case may not be applicable for other cases. To understand the general
74 relationships between SCM phenomenon and environmental parameters, the
75 analytical solution for dynamic ecosystem equations is needed.

76 The algae game theoretical model, pioneered by Klausmeier and Litchmann (2001),
77 was perhaps the first one to derive the depth and intensity of SCML, although the
78 SCML is assumed to be infinitely thin. They adopted a delta function to approximate
79 the phytoplankton distribution in this thin layer. Yoshiyama et al. (2009) used this
80 model to examine more than one species competing for limiting nutrients and light
81 below the surface mixed layer. Mellard et al. (2011) included stratification into this
82 model. However, the SCML was still confined to an infinitely thin layer. In fact,
83 many observations showed that the thickness of SCML can reach as high as 100 m in
84 oceans (Platt et al., 1988). For those cases, the assumption of an infinitely small
85 thickness of SCML is contradictory to the observations.

86 In this study, we assume that the vertical profile of Chl a can be approximately treated
87 as a general Gaussian function, instead of a delta function. This parameterizing
88 approach was proposed firstly by Lewis et al. (1983), and has been widely used to fit
89 vertical profiles of Chl a (Platt et al., 1988; Weston et al., 2005; Ardyna et al., 2013).

90 By incorporating the general Gaussian function into the ecosystem dynamical
91 equations, we derive the steady-state solutions for the thickness, depth, and intensity
92 of SCML in various scenarios and examine their dependence on environmental
93 parameters, such as light attenuation coefficient, vertical diffusivity, sinking velocity
94 of phytoplankton.

2 Methods

2.1 Models

97 The SCML occurs below the surface mixed layer, where the light attenuated from
98 above and nutrients supplied from the deep water result in the maximal value of
99 phytoplankton growth rate (Fig. 1). The partial differential equations for
100 phytoplankton and nutrients dynamics in which light and nutrients are two major
101 limiting factors (Eqs. 1 and 2) (Riley et al., 1949; Lewis et al., 1986; Gabric and
102 Parslow, 1989; Huisman et al., 2006; Liccardo et al., 2013) were adopted in this
103 study.

$$\frac{\partial P}{\partial t} = \mu_m \min\big(f(I), g(N)\big)P - \varepsilon P - w\frac{\partial P}{\partial z} + \frac{\partial}{\partial z}\left(K_v \frac{\partial P}{\partial z}\right), \tag{1}$$

$$\frac{\partial N}{\partial t} = -1.59\mu_m \min\big(f(I), g(N)\big)P + 1.59\alpha\varepsilon P + \frac{\partial}{\partial z}\left(K_v \frac{\partial N}{\partial z}\right), \tag{2}$$

106 where P denotes the Chl a concentration, N is the limiting nutrient concentration. The
107 photo-acclimation of phytoplankton is not considered here and the Chl a distribution
108 is supposed to represent the distribution of phytoplankton biomass. This is a
109 significant simplification. In fact, phytoplankton increases inter-cellular pigment
110 concentration when light level decreases (Cullen, 1982; Fennel and Boss, 2003).
111 Usually, the unit of Chl a concentration is mg m^{-3}, the concentrations of
112 phytoplankton and the limiting nutrients are in unit of mmol N m^{-3}. A ratio of 1.59 g
113 chlorophyll per mol nitrogen (Cloern et al., 1995; Oschlies, 2001) is thereby used for
114 unit conversion. μ_m is the maximum growth rate of phytoplankton, ε is the loss
115 rate of phytoplankton (including respiration, mortality, zooplankton grazing), α is
116 the recycling rate of dead phytoplankton ($0 \le \alpha \le 1$). w is the sinking velocity of
117 phytoplankton, which is non-negative in the chosen coordinate system and assumed
118 to be constant with depths. K_v is the vertical turbulent diffusivity and it is much

119 larger within the surface mixed layer than that beneath. Here, K_v depends on depth

120 in the following way (Hodges and Rudnick, 2004; Mellard et al., 2011):

$$K_v = \begin{cases} K_{v1} & 0 < z < z_s, \\ K_{v2} & z_s < z < z_b, \end{cases} \tag{3}$$

122 where z_s is the depth of surface mixed layer, z_b is the location where the Chl a

123 concentration reduces to nearly zero in a sufficiently deep water column. We assume

124 K_{v1}, K_{v2} are constant and K_{v1} is large enough to homogenize the Chl a and nutrient

125 concentrations in the surface mixed layer.

126 A gradual transition from the surface mixed layer to the deep one written in terms of a

127 generalized Fermi function is adopted (Ryabov et al., 2010), that is, $K_v(z) = K_{v2} +$

128 $\frac{K_{v1}-K_{v2}}{1+e^{(z-z_s)/l}}$, where parameter l characterizes the width of the transition layer. In our

129 study, we assumed this transition layer is finitely thin.

130 The growth limited function $\min\big(f(I), g(N)\big)$ for light I and nutrients N is:

$$\min\big(f(I), g(N)\big) = \min\left(\frac{I(z)}{K_I + I(z)}, \frac{N(z)}{K_N + N(z)}\right), \tag{4}$$

132 where K_I and K_N denote the half-saturation constants of light and nutrients,

133 respectively. The net growth rate, $\mu_m \min\big(f(I), g(N)\big) - \varepsilon$, is positive only if both the

134 light limiting term $\mu_m f(I)$ and nutrient limiting term $\mu_m g(N)$ are larger than the

135 loss rate ε.

136 Light intensity is assumed to decrease exponentially with depth according to

137 Lambert-Beer's law, i.e.,

$$I(z) = I_0 \exp\big(-K_d z\big), \tag{5}$$

139 where I_0 is the surface light intensity and K_d is the light attenuation coefficient (Morel,

140 1988). Assuming a constant K_d, we ignore the effects of the self-shading and the

141 dissolved and particulate material on the attenuation coefficient.

142 The zero-flux boundary condition for the phytoplankton at the surface is used. Like

143 the study reported by Ryabov et al. (2010), we also set the chlorophyll concentration

144 approaches zero at the bottom boundary z_b, i.e., $P \rightarrow 0$ for $z \rightarrow z_b$. Fennel and Boss

145 (2003) used an infinite depth as z_b. Furthermore, we assume a zero-flux boundary

146 condition for nutrients at the surface, while nutrients are replenished from below.

147 That is,

148
$$\begin{cases} K_{v1}\dfrac{\partial P}{\partial z} = 0, & K_{v1}\dfrac{\partial N}{\partial z} = 0, & at \ z = 0, \\ P(z_b) = 0, & K_{v2}\dfrac{\partial N}{\partial z} = K_{v2}\dfrac{\partial N}{\partial z}\Big|_{z=z_b}, & at \ z = z_b. \end{cases} \tag{6}$$

149 In addition, Lewis et al. (1983) first proposed a general Gaussian distribution function

150 (Eq. 7) to model the nonlinear feature of observed vertical Chl a profiles. In this study,

151 this function is adopted to represent the bell-shape vertical distribution of Chl a (Fig.

152 1).

153
$$P(z) = P_{max}e^{-\frac{(z-z_m)^2}{2\sigma^2}} \quad 0 \le z \le z_b, \tag{7}$$

154 where $P(z)$ is Chl a concentration as a function of depth z, and $P_{max} = \dfrac{h}{\sigma\sqrt{2\pi}}$. The

155 three Gaussian parameters (h, z_m, σ) can vary to characterize the SCM phenomenon.

156 Thus h is the vertical integrated Chl a over the entire water column, z_m is the depth of

157 the maximum Chl a (the peak of the bell-shape), and σ is the standard deviation of

158 Gaussian function, which controls the thickness of the SCML.

159 *2.2 Three SCM characteristics*

160 The thickness of SCML can characterize the vertical extent of Chl a distribution

161 below the surface mixed layer. It is still debatable how to best define the thickness of

162 SCML. One easy definition is to use the width between two locations below and

163 above the Chl a peak, where Chl a is a certain fraction (e.g. 50%, $100(e^{-1/2})$%) of the

164 maximum Chl a (Platt et al., 1988; Pérez et al., 2006). Some studies bounded the

165 layer by sharp vertical gradients in Chl a above and below the peak (Prairie et al.,

166 2011). Others defined the upper and lower boundary of SCML by ad hoc choices.

167 Pedrós-Alió et al. (1999) proposed the SCML from the depth of the surface mixed

168 layer to the lower maximum gradient in the slope of the Chl a profile. Hanson et al.

169 (2007) defined that the upper boundary of the SCML was the minimum gradient

170 criterion of 0.02 mg Chl a m^{-1} and the lower was the base of the euphotic zone.

171 Beckmann and Hense (2007) proposed to define the boundaries of SCML by the

172 existence of two community compensation depths in the water column, which were

173 located at the depths of two maximum phytoplankton gradients in phytoplankton

174 biomass.

175 Building on the study by Beckmann and Hense (2007), the locations of the maximum

176 phytoplankton gradients are defined as the boundaries of SCML in this study. That is,

177
$$\frac{d^2P}{dz^2}\bigg|_{z=z_u,z_l} = 0, \tag{8}$$

178 where z_u and z_l are the upper and lower boundary of SCML, respectively.

179 By substituting Eq. (7) into this equality, we obtain $z_u = z_m - \sigma$, $z_l = z_m + \sigma$. Thus,

180 the thickness of SCML can thereby be expressed as 2σ.

181 From Eq. (8) and the steady state of Eq. (1), one gets the following equality at the

182 boundaries of SCML:

183
$$\left(\mu_m \min\left(f(I), g(N)\right) P - \varepsilon P - w\frac{dP}{dz} \right)\bigg|_{z=z_u,z_l} = 0. \tag{9}$$

184 That is, the boundary of SCML is located at the depth where there is the balance

185 between phytoplankton growth and all losses (including the divergence of the sinking

186 flux $w\frac{dP}{dz}$ and the loss ε due to mortality, respiration, and grazing), named the

187 community compensation depth (Ono et al., 2001). Thus, this definition reflects the

188 physical-biological ecosystem dynamics associated with SCML.

189 As described in Eq. (7), the depth of the SCML is defined as z_m, that is, the location

190 of the point-wise maximum value of Chl a.

191 The third quantity, i.e. the intensity of SCML, refers to the maximum value of Chl a

192 (P_{max} in Eq. 7) in the water column.

193 *2.3 Approach used in this study*

194 Previous numerical studies (Huisman et al., 2006; Ryabov et al., 2010) showed that

195 the ecosystem dynamical model (Eqs. 1 and 2) can approximately reproduce the

196 bell-shape feature of the vertical Chl a profile (Fig. 1). We assume a general

197 Gaussian function of $P(z)$ (Eq. 7) is the solution for the Eqs. (1) and (2) at

198 steady-state to derive explicit relationships between three characteristics of SCM and

199 the environmental parameters. If nutrient input to the mixed layer due to riverine

200 inputs, surface runoff, or atmospheric deposition, is considered in the ecosystem, the

201 surface concentration of Chl a should be positive (Mellard et al. 2011). Thus, the

202   general Gaussian function is not an exact solution, at best, an approximate solution of

203   the dynamical Eqs. (1) and (2) by ignoring external nutrient input.

204   Firstly, by substituting the general Gaussian function of $P(z)$ with the steady-state

205   version of Eq. (1), we obtain that below the surface mixed layer the net growth rate of

206   phytoplankton can be expressed as follows

207
$$\mu_m \min\left(f(I), g(N)\right) - \varepsilon = -\frac{K_{v2}}{\sigma^4}\left(z - z_m + \frac{w\sigma^2}{2K_{v2}}\right)^2 + \frac{w^2}{4K_{v2}} + \frac{K_{v2}}{\sigma^2}. \tag{10}$$

208   Letting $\mu_m \min\left(f(I), g(N)\right) - \varepsilon = 0$, we get the two compensation depths, z_{c1}, z_{c2},

209   by solving Eq. (10):

210
$$z_{c1} = z_m - \frac{w\sigma^2}{2K_{v2}} - \sqrt{\left(\frac{w\sigma^2}{2K_{v2}}\right)^2 + \sigma^2}, \; z_{c2} = z_m - \frac{w\sigma^2}{2K_{v2}} + \sqrt{\left(\frac{w\sigma^2}{2K_{v2}}\right)^2 + \sigma^2}. \tag{11}$$

211   From the property of quadratic function with pointing downward (the right-hand

212   terms in Eq. 10), we know that for $z_{c1} < z < z_{c2}$ the inequality

213     $\mu_m \min(f(I), g(N)) - \varepsilon > 0$ is satisfied. This indicates that the subsurface net production

214   occurs only between the two compensation depths where the growth rate

215     $\mu_m \min(f(I), g(N))$ equals the loss rate ε. Beckmann and Hense (2007) found similar

216   results by numerical modeling and emphasized the often overlooked fact that an

217   SCML has to have two compensation depths.

218   From Eq. (11), we obtain $z_{c1} \leq z_m - \sigma$ and $z_m \leq z_{c2} \leq z_m + \sigma$ (Fig. 1). In particularly,

219     $z_{c1} = z_m - \sigma$, and $z_{c2} = z_m + \sigma$ when the sinking velocity of phytoplankton w is too

220   small to affect the chlorophyll profile significantly. This result is identical to that of

221   Beckmann and Hense (2007) for neglecting sinking velocity of phytoplankton.

222   Hence, according to the property of quadratic function, there exists a depth z_0

223   between the two compensation depths,

224
$$z_0 = z_m - \frac{w\sigma^2}{2K_{v2}}, \tag{12}$$

225   such that the net growth rate of phytoplankton is at its maximum, i.e.,

226
$$\max\left(\mu_m \min\left(f(I), g(N)\right) - \varepsilon\right)\Big|_{z_0} = \frac{K_{v2}}{\sigma^2} + \frac{w^2}{4K_{v2}}. \tag{13}$$

227   In other words, the maximum in net growth rates of phytoplankton occurs at the
228   depth of z_0.

229   We define $T = \sigma^2 / K_{v2}$ as the characteristic vertical mixing time scale in the SCML of
230   thickness σ (Bowdon, 1985; Gabric and Parslow, 1989). Let the length scale be
231    $L = 2K_{v2}/w$, which determines the scale height of the phytoplankton distribution
232   (Ghosal and Mandre, 2003). Thus, the right hand terms of Eq. (13) can be rewritten
233   as $1/T + w/(2L)$. In other words, the maximum net growth rate of phytoplankton,
234    $\max(\mu_m \min(f(I), g(N)) - \varepsilon)$, is determined by the vertical mixing time scale (T) and the
235   time taken by a phytoplankton sinking (w) through lengths ($2L$).

236   Equation (12) also shows that $z_m \geq z_0$, that is, the depth of SCML lies at or below
237   the depth for phytoplankton having the maximum growth rate. Observations in the
238   Southern California Bight have supported this (Cullen and Eppley, 1981).
239   Particularly, $z_m = z_0$ approximately holds when either the sinking velocity (w) or
240   Gaussian parameter σ is very small. For non-sinking phytoplankton, i.e., $w \rightarrow 0$,
241   numerical modeling can support this equality (Beckmann and Hense, 2007). When
242   parameter σ is assumed to be infinitely thin, the equality is obviously correct, which
243   has been used to solve for the equilibrium depth and intensity of an infinitely thin
244   layer (Klausmeier and Litchman, 2001; Yoshiyama et al., 2009; Mellard et al., 2011).

245   In this special case ($z_m = z_0$), some studies found that the depth of SCML is at the
246   location of equal limitation by nutrients and light (Klausmeier and Litchman, 2001;
247   Yoshiyama et al., 2009; Mellard et al., 2011). In this study, we further infer that when
248    $z_m > z_0$, the depth of SCML is located at where phytoplankton growth is limited by
249   light (Appendix A).

250   According to Eqs. (12) and (A2), the growth of phytoplankton is light-limited at and
251   below the depth of SCML. Therefore, for $z = z_m$ and $z = z_m + \sigma$, the net growth rate
252   of phytoplankton (Eq. 10) can be expressed as following, respectively:

253
$$\mu_m f(I)\big|_{z=z_m} - \varepsilon = K_{v2}\big/\sigma^2$$
(14)

254
$$\mu_m f(I)\big|_{z=z_m+\sigma} - \varepsilon = -w\big/\sigma$$
(15)

255   At the depth of z_m, the net growth rate of phytoplankton (Eq. 14) is determined by

256   the vertical mixing time, T, while the time taken by phytoplankton sinking through

257   half-length of SCML, w/σ, controls the net growth rate of phytoplankton (Eq. 15) at

258   the lower boundary of SCML ($z_m + \sigma$).

259   In addition, from Eqs. (12) and (A2) we obtain that the upper compensation depth, z_{c1},

260   is the location where the growth limited by nutrients, $\mu_m g(N)$, equals the loss rate,

261   ε, while the lower compensation depth, z_{c2}, represents the depth where the growth

262   limited by light, $\mu_m f(I)$, equals the loss rate, ε.

263   **3 Results**

264   *3.1 Analytic solutions of three SCM characteristics*

265   By substituting the growth limitation function for light (Eqs. 4 and 5) into Eqs. (14)

266   or (15), we obtain the expression of parameter z_m, i.e.,

267
$$z_m = \frac{1}{K_d} \ln\left[\left(\frac{\mu_m}{\varepsilon + K_{v2}/\sigma^2} - 1\right)\frac{I_0}{K_I}\right] \tag{16}$$

268   or

269
$$z_m = \frac{1}{K_d} \ln\left[\left(\frac{\mu_m}{\varepsilon - w/\sigma} - 1\right)\frac{I_0}{K_I}\right] - \sigma. \tag{17}$$

270   The occurrence for a SCM requires $z_m > 0$. Requiring a positive solution for Eq.

271   (16), we obtain $\left(\frac{\mu_m}{\varepsilon + K_{v2}/\sigma^2} - 1\right)\frac{I_0}{K_I} > 1$, i.e., $\left(\mu_m f(I_0) - \varepsilon\right)\sigma^2 > K_{v2}$. For any $\sigma > 0$, we

272   get $\mu_m f(I_0) > \varepsilon$. That is, the necessary condition for the existence of SCM is

273    $\mu_m f(I_0) > \varepsilon$, which is identical with the result of Fennel and Boss (2003) when

274   vertical sinking is constant as a function of depth in their model.

275   Subtracting Eqs. (16) and (17), and rearranging, we obtain the expression of

276   parameter σ:

277
$$\left(\frac{\mu_m}{\mu_m - \varepsilon + \dfrac{w}{\sigma}} - 1\right)e^{K_d\sigma} = \frac{\mu_m}{\mu_m - \varepsilon - \dfrac{K_{v2}}{\sigma^2}} - 1 \tag{18}$$

278   Thus far, we have obtained the theoretical relationships between Gaussian parameter

279   σ, z_m and environmental parameters (Eqs. 16-18). To derive the relationship between

280   Gaussian parameter h and environmental parameters, we now return to Eqs. (1) and

281   (2). In steady state, adding these two equations leads to:

$$(1-\alpha)\varepsilon P + w\frac{dP}{dz} = \frac{d^2(K_v P)}{dz^2} + \frac{1}{1.59}\frac{d^2(K_v N)}{dz^2} \tag{19}$$

283   Note that this relationship holds irrespective of the form of growth limiting function.

284   Integrating this equation from the surface to bottom boundary (z_b) and using

285   boundary conditions (Eq. 6) gives:

$$1.59(1-\alpha)\varepsilon\int_0^{z_b} P(z)dz = K_{v2}\frac{dN}{dz}\Big|_{z=z_b} \tag{20}$$

287   When the recycling processes do not immediately convert dead phytoplankton back

288   into dissolved nutrients below the surface mixed layer, i.e., $\alpha \neq 1$ (For $\alpha = 1$, the

289   detailed derivation for the intensity of SCML is presented at Appendix B), one gets

290   the total Chl a in the water column:

$$h = \frac{K_{v2}\frac{dN}{dz}\Big|_{z=z_b}}{1.59(1-\alpha)\varepsilon} \tag{21}$$

292   This equality indicates that the total Chl a in the water column (h) is independent of

293   the sinking velocity of phytoplankton. Both Ryabov et al. (2010) and Mellard et al.

294   (2011) obtained a similar result.

295   The intensity of SCML is

$$P_{\max} = \frac{K_{v2}\frac{dN}{dz}\Big|_{z=z_b}}{1.59\sqrt{2\pi}\sigma(1-\alpha)\varepsilon} \tag{22}$$

297   Obviously, both the total Chl a in the water column and the intensity of SCML are

298   proportional to the flux of nutrients from below ($K_{v2}\frac{dN}{dz}\Big|_{z=z_b}$), which is determined

299   by the diffusivity below the surface mixed layer and the nutrients gradient at the

300   bottom of water column. Varela et al. (1994) also found a similar result by

301   simulations.

302   *3.2 Influences of environmental parameters on SCM characteristics*

303   We now investigate how the steady-state thickness, depth, and intensity of SCML

304   depend on environmental parameters. Because the analytic solutions for SCML depth

305   and intensity depend on Gaussian parameter σ and environmental parameters, we first

306   examine the influence of environmental parameters on parameter σ.

307   Equation (18) shows that the thickness of SCML is independent of sea surface light

308   intensity (I_0). This is consistent with numerical simulations (Beckmann and Hense,

309   2007). This result also suggests that seasonal variation of SCML thickness has no

310   relation with light intensity. Thus, it is not surprising that the empirical model poorly

311   predicted parameter σ by using season as an important factor (Richardson et al.,

312   2003).

313   To illustrate the effects of other model parameters (K_d, K_{v2}, μ_m, ε, w) on the parameter

314   σ, we need to obtain informative algebraic expression of σ. To simplify, by Taylor

315   expanding $e^{K_d\sigma}$ at $\sigma=0$ and truncating the Taylor series after the linear term, i.e.,

316    $e^{K_d\sigma}=1+K_d\sigma+o(\sigma^2)$, Eq. (18) can thereby be rewritten as:

317
$$\sigma^3 - \frac{w}{\varepsilon}\sigma^2 - \frac{\varepsilon K_d K_{v2}+\mu_m w}{\varepsilon K_d(\mu_m-\varepsilon)}\sigma = \frac{K_{v2}(\mu_m/K_d-w)}{\varepsilon(\mu_m-\varepsilon)}. \tag{23}$$

318   According to the properties of a cubic function, we know that Eq. (23) has one and

319   only one positive real root σ, when $\dfrac{K_{v2}(\mu_m/K_d-w)}{\varepsilon(\mu_m-\varepsilon)}\geq 0$. Because $\mu_m f(I_0)>\varepsilon$ and

320    $0<f(I_0)<1$, so $\mu_m>\varepsilon$. Thus, when the maximum phytoplankton growth rate (μ_m)

321   within one penetration depth ($1/K_d$) is larger than sinking velocity of phytoplankton,

322   i.e., $\mu_m/K_d-w\geq 0$, there exists a non-negative value of parameter σ, which

323   increases with increasing $\dfrac{K_{v2}(\mu_m/K_d-w)}{\varepsilon(\mu_m-\varepsilon)}$.

324   Using dimensional analysis, Klausmeier and Litchman (2001) found that the degree

325   of turbulence determines the thickness of SCML. Our analytical result shows that the

326   thickness of SCML increases with increasing vertical diffusivity below the surface

327   mixed layer (K_{v2}). In addition, the SCML thickness decreases with increasing sinking

328   velocity of phytoplankton (w) and light attenuation coefficient (K_d).

329   The right hand term in Eq. (23), $\dfrac{K_{v2}(\mu_m/K_d-w)}{\varepsilon(\mu_m-\varepsilon)}$, can be rearranged as

330    $\dfrac{K_{v2}(\mu_m/K_d-w)}{-(\varepsilon-\mu_m/2)^2+\mu_m^2/4}$. Thus, the effect of loss rate (ε) on parameter σ depends on $\mu_m/2$.

331   Note that $\mu_m f(I_0) > \varepsilon$ once the SCM occurs. When the surface light intensity I_0 is

332   smaller than or equals to the half-saturation constant for light K_I, i.e., $f(I_0) \leq 0.5$,

333   then $0 < \varepsilon < \mu_m f(I_0) \leq \mu_m/2$, thus, σ decreases with increasing ε. Conversely, when

334      $f(I_0) > 0.5$, for $\varepsilon \geq \mu_m/2$, σ increases with increasing ε; for $\varepsilon < \mu_m/2$, σ decreases

335   with increasing ε. In summary, for smaller loss rates ($\varepsilon < \mu_m/2$), decreased ε leads to

336   a thicker SCML, while for larger loss rates ($\varepsilon \geq \mu_m/2$), decreased ε leads to a thinner

337   SCML.

338   Equation (16) can be rewritten as:

339
$$z_m = \frac{1}{K_d} \ln(A I_0), \tag{24}$$

340   where $A = \frac{1}{K_I}\left(\frac{\mu_m}{\varepsilon + K_{v2}/\sigma^2} - 1\right)$. Clearly, from Eq. (18) we know A does not depend on

341   surface light intensity (I_0), thus we infer that the depth of SCML increases

342   logarithmically with increasing I_0. In other words, the SCML gets deeper due to the

343   seasonal increase of I_0, and remains almost unchanged when the surface light

344   intensity increases to a certain degree. Observations at the HOT (Hawaii Ocean

345   Time-series) site in the eastern Pacific and the SEATS (South East Asia Time-series

346   Station) station in the South China Sea showed a significant seasonal variation of

347   SCML depth (Chen et al., 2006; Hense and Beckmann, 2008). Hense and Beckmann

348   (2008) explained the deepening of SCML depth in spring at HOT site by the seasonal

349   increase of the light intensity. Modeling sensitivity analyses also showed that an

350   increase in the surface light intensity yields a deeper SCML (Jamart et al., 1979;

351   Varela et al., 1994; Beckmann and Hense, 2007).

352   Determining the effect of vertical diffusivity below the surface mixed layer (K_{v2}) on

353   the steady-state SCML intensity is more difficult. Increased K_{v2} increases parameter

354   σ (Eq. 23) and the diffusive flux of nutrients from below (Eq. 22), however, this

355   parameter has opposite effects on P_{max} (Eq. 22). Rearranged Eq. (23) we obtain

356
$$\frac{K_{v2}}{\sigma} = \frac{(\mu_m - \varepsilon)\varepsilon}{(\mu_m/K_d - w)/\sigma^2 + \varepsilon/\sigma} + \frac{(\mu_m - \varepsilon)w}{(\mu_m/K_d - w)/\sigma + \varepsilon} - \frac{\mu_m w/K_d}{\mu_m/K_d - w + \varepsilon\sigma}. \tag{25}$$

357   Clearly, all the three terms in the right hand of this equality increase due to the

358   increasing σ by a higher K_{v2}. Therefore, it can be inferred that increased vertical

359 diffusivity below the surface mixed layer (K_{v2}) leads to a stronger SCML intensity

360 (P_{max}).

361 The influences of various parameters on SCM characteristics determined by Eqs.

362 (16)-(18), (21) and (22) are summarized in Table 1. For example, increased light

363 levels (increasing surface light intensity I_0, decreasing attenuation coefficient K_d) or

364 increased light competitive ability (decreasing half-saturation constant for light K_I)

365 moves the SCML deeper; increased nutrients supply (increasing vertical diffusivity

366 below the surface mixed layer K_{v2} and loss rate of phytoplankton ε) moves the layer

367 toward the surface. The shape of SCML (thickness and intensity) is mainly

368 influenced by nutrients supply (K_{v2} and ε). The intensity of SCML becomes weaker

369 as a result of expanding the SCML by a lower sinking velocity of phytoplankton (w)

370 and a smaller light attenuation coefficient (K_d).

371 **4 Discussion**

372 Considering the two compartment system (nutrients and Chl a) in steady state and a

373 general Gaussian function for vertical Chl a concentration, we derived the analytical

374 solution for the fundamental relationships between SCM characteristics and various

375 parameters. Three special scenarios, limitation and implications of this study were

376 discussed below.

377 *4.1 Three special scenarios*

378 Equation (18) indicates that the parameter σ is affected by changes in the vertical

379 diffusivity below the surface mixed layer (K_{v2}), the sinking velocity of phytoplankton

380 (w) and the light attenuation coefficient (K_d), which inversely affects depth and

381 intensity of SCML (Eqs. 16, 17, and 22). Thus, three special situations of the

382 theoretical solutions for SCM characteristics are discussed below.

383 Firstly, the term K_{v2}/σ^2 in the right hand of Eq. (18) is neglected. This special

384 situation occurs either when the vertical diffusivity below the surface mixed layer is

385 too small to be considered ($K_{v2} \rightarrow 0$), or when K_{v2}/σ^2 is much smaller than $\mu_m - \varepsilon$,

386 i.e., the mixing time scale ($T = \sigma^2/K_{v2}$) below the surface mixed layer is much longer

387 than the time taken by net growth of phytoplankton, $(\mu_m - \varepsilon)^{-1}$. Indeed, in the

388 seasonal thermocline, vertical turbulent diffusive time scales can vary from weeks to

389 months for phytoplankton displacements as small as several meters (Denman and

390   Gargett, 1983). The value of $(\mu_m - \varepsilon)^{-1}$ used in many studies is usually from 0.1 to 5

391   days (Gabric and Parslow, 1989; Klausmeier and Litchman, 2001; Huisman et al.,

392   2006).

393   In this situation, from Eq. (14), the growth rate at SCML depth can be expressed as:

394

$$\mu_m f(I)|_{z=z_m} = \varepsilon. \tag{26}$$

395   In regions with a low vertical diffusivity, Fennel and Boss (2003) derived that, at the

396   SCML depth, the growth rate of phytoplankton is equal to the loss rate and the

397   divergence of phytoplankton due to changes in the sinking velocity. Clearly, Eq. (26)

398   is identical to that of Fennel and Boss (2003) for constant sinking velocity of

399   phytoplankton.

400   In this situation, the depth of SCML can be derived from Eq. (16), i.e.,

401

$$z_m = \frac{1}{K_d} \ln \frac{(\mu_m - \varepsilon) I_0}{\varepsilon K_I}. \tag{27}$$

402   It indicates the SCML depth is directly proportional to the light penetration depth

403   ($1/K_d$). Observations by four Bio-Argo floats in the North Pacific Subtropical Gyre,

404   the South Pacific Subtropical Gyre, the Levantine Sea, and in the northwestern

405   Mediterranean Sea showed a significant positive linear relationship between the two

406   variables (Mignot et al. 2014). Beckmann and Hense (2007) also found a similar

407   result by statistical analysis of numerical modeling.

408   The right hand term of Eq. (27) can be rewritten as $\frac{1}{K_d} \ln \frac{I_0}{I^*}$ by letting $I^* = \frac{\varepsilon K_I}{\mu_m - \varepsilon}$,

409   where $\mu_m f(I^*) = \varepsilon$. Under the assumption of infinitely thin SCML ($\sigma \to 0$),

410   Klausmeier and Litchman (2001) also have derived Eq. (27) by setting the vertical

411   diffusivity for phytoplankton as zero, i.e., $K_v = 0$, in poorly mixed waters. Here, we

412   go further to obtain the approximate expression of the thickness of SCML from Eq.

413   (23), that is,

414

$$2\sigma = \frac{w}{\varepsilon} + \sqrt{\left(\frac{w}{\varepsilon}\right)^2 + \frac{w}{K_d \left(\varepsilon - \varepsilon^2 / \mu_m\right)}}. \tag{28}$$

415   Obviously, the thickness of SCML increases with an increase in the sinking velocity

416   of phytoplankton (w), and with a decrease in the maximal growth rate (μ_m) and the

417   light attenuation coefficient (K_d).

418   The second special situation occurs when the term w/σ in the left hand of Eq. (18) is

419   neglected. This special case occurs in regions where phytoplankton sinking velocity

420   is very low ($w \rightarrow 0$), or when w/σ is much smaller than $\mu_m - \varepsilon$, i.e., the time taken by

421   phytoplankton sinking through half-length of SCML, $(w/\sigma)^{-1}$, is much longer than the

422   time taken by net growth of phytoplankton, $(\mu_m - \varepsilon)^{-1}$. Phytoplankton sinking

423   velocities exhibit a range of values depending on physical and physiological

424   phenomena (e.g., size and shape of the cell). In the environment, estimates of sinking

425   velocity vary from 0 to 9 m per day (Gabric and Parslow, 1989; Huisman and

426   Sommeijer, 2002). Thus, the latter special scenarios (i.e., $w/\sigma \ll \mu_m - \varepsilon$) can indeed

427   occur.

428   In this situation, according to Eq. (15), the net growth rate at the lower boundary of

429   SCML can be expressed as

430
$$\mu_m f(I)\big|_{z=z_m+\sigma} - \varepsilon = 0. \tag{29}$$

431   That is, the lower boundary of SCML, $z_m+\sigma$, is located at the compensation depth.

432   In this situation, the depth of SCML can be derived from Eq. (17), i.e.,

433
$$z_m = \frac{1}{K_d} \ln \frac{(\mu_m - \varepsilon)I_0}{\varepsilon K_I} - \sigma. \tag{30}$$

434   Compared with Eq. (27), we know that the depth of SCML is shallower in this special

435   case than that in the case of neglecting the influence of vertical diffusivity below the

436   surface mixed layer on SCM. This result implies that the displacement (σ) of SCML

437   depth is the result of combined influences of vertical diffusivity and sinking velocity

438   of phytoplankton.

439   In this situation, from Eq. (23), we have

440
$$\sigma\left(\sigma + \sqrt{\frac{K_{v2}}{\mu_m - \varepsilon}}\right)\left(\sigma - \sqrt{\frac{K_{v2}}{\mu_m - \varepsilon}}\right) = \frac{\mu_m K_{v2}}{(\mu_m - \varepsilon)\varepsilon K_d}. \tag{31}$$

441   The SCML thickens with a larger vertical diffusivity below the surface mixed layer

442   (K_{v2}), a smaller growth rate (μ_m) or a lower light attenuation coefficient (K_d).

443 Especially, when $K_{v2}=0$, we have $\sigma=0$. In other words, for non-sinking

444 phytoplankton ($w\rightarrow 0$), when the vertical diffusivity below the surface mixed layer is

445 very small ($K_{v2}\rightarrow 0$), the SCML disappears. This indicates that there must be a

446 vertical diffusion window sustaining non-sinking phytoplankton species in deep

447 waters.

448 The third special situation occurs when $K_d\sigma$ (i.e., $\sigma/\left(K_d\right)^{-1}$) is too small to be

449 considered in Eq. (18). This may occur in clear waters where the light attenuation

450 coefficient is very small ($K_d\rightarrow 0$), or in regions where the light penetration depth

451 ($1/K_d$) is much larger than a half-width of SCML (σ). Very narrow (from several to

452 tens of centimeters) SCML has been observed in clear, stratified lakes where the light

453 penetration depths were from several to tens of meters (Fee, 1976; Camacho, 2006).

454 In this situation, Eq. (18) can be modified to

$$w\sigma + K_{v2} = 0. \tag{32}$$

456 Clearly, when $K_{v2}=0$, $w=0$, this equation has infinitely many solutions. This means

457 in stable, clear waters with a predominance of small cells, the deep SCML can occur

458 with different thicknesses. For example, in the basin of South China Sea, <3 μm

459 phytoplankton (such as *Prochlorococcus, Synechococcus*, picoeukaryotes, etc.) are

460 the dominant species in SCMLs (Takahashi and Hori, 1984; Liu et al., 2007) with

461 variable thicknesses (Lee Chen, 2005; Chen et al., 2006).

462 *4.2 Limitation and potential application*

463 To make the complex problem (SCM phenomenon) tractable, the ecosystem

464 dynamical equations adopted in this study are judiciously simplified. For example, a

465 constant eddy diffusivity is assumed in the surface mixed layer and below this layer,

466 respectively. Many processes (turbulence, internal waves, storms, slant-wise and

467 vertical convection) in upper ocean dynamics are not captured in the model system.

468 The assumption of steady state will be broken during episodic events of strong

469 physical forcing, nutrient injection, or blooms (Fennel and Boss, 2003). Similarly the

470 biological representation is also extremely limited. We neglect food-web and

471 microbial loop dynamics (detritus, dissolved organic matter, and zooplankton are not

472 included explicitly), and assume all loss processes, except sinking, to be linearly

473 proportional to phytoplankton. The sinking velocity of phytoplankton is assumed to

474   be constant with depths, excluding the effects of temperature and density gradients.

475   Our model also neglects some feedback mechanisms, like the effect of phytoplankton

476   on light attenuation. Although these are important aspects, their addition is unlikely to

477   change our conclusions qualitatively under the boundary conditions chosen in this

478   study (Fennel and Boss, 2003).

479   Without considering nutrient input directly to the surface mixed layer, phytoplankton

480   within it is assumed to be nearly zero. This assumption has been proved by Mellard

481   et al. (2011). The SCML is assumed to occur significantly deeper than the base of

482   surface mixed layer, and the vertical gradient of phytoplankton is assumed to be

483   identically zero at the transition between the two layers. This vertical profile of

484   phytoplankton (Fig. 1) is assumed to be fitted by a general Gaussian function (Eq. 7),

485   in which phytoplankton within the surface mixed layer is an approximation for the

486   tail of Gaussian function. The Gaussian assumption leads to the results that both

487   phytoplankton concentration and vertical diffusivity within the surface mixed layer

488   have no roles on the SCM. However, the assumption of a general Gaussian profile

489   can be broken in several ways. If nutrient input directly to the mixed layer due to

490   riverine inputs, surface runoff, or atmospheric deposition, Chl a concentration within

491   the surface mixed layer will be sustained, while a SCM by itself will be not possible

492   (Mellard et al. 2011). If the depth of surface mixed layer z_s is large, this allows

493   another way for the surface Chl a concentration being positive by extracting some of

494   the Chl a from the SCML (Beckman and Hense, 2007), then the vertical gradient of

495   Chl a may not be identically zero at the transition between the two layers.

496   Under the assumption of a constant loss rate, the lower compensation depth we got

497   from Eq. (11), the location where the growth rate of phytoplankton limited by light

498   equals the loss rate, is similar to the popular definition of compensation depth given

499   by Sverdrup (1953), below which no net growth occurs. This assumption is in the

500   heart of the Sverdrup's critical depth model and we now understand that it has

501   significant limitations (Behrenfeld and Boss, 2014). Particularly, the treatment of

502   grazing loss, is, in the least, an oversimplification, though many numerical models

503   used a similar one (e.g., Klausmeier and Litchman, 2001; Fennel and Boss, 2003;

504   Huisman et al., 2006). Grazing loss depends strongly on phytoplankton and

505   zooplankton concentrations (it is an encounter based process) and, given that

506   zooplankton can move, or, in the least, grow faster where more food is available, is

507   unlikely to have a constant concentration distribution (Behrenfeld and Boss, 2014).

508   Our model suggests that the condition for the existence of a SCM is that the growth

509   rate under the limitation of light intensity, $\mu_m f(I_0)$, is larger than the loss rate, ε, in

510   stratified water columns. Fennel and Boss (2003) found a similar result and pointed

511   out that this condition for a SCM is general. Many numerical studies have reproduced

512   the SCM phenomenon, of which the condition of SCM occurrence met with variable

513   values of the sinking velocity of phytoplankton and the mixing diffusivity

514   (Klausmeier and Litchman, 2001; Huisman et al., 2006; Mellard et al., 2011).

515   Our two compartment system model reproduces some of the results of the more

516   complex model with three compartments (phytoplankton, nutrients, and detritus,

517   Beckmann and Hense, 2007). For example, our model predicts that with fully

518   recycling of the dead phytoplankton, the total Chl a concentration in water columns

519   depends on the sinking velocity of phytoplankton and the vertical diffusivity, but

520   independents on the growth rate and the loss rate of phytoplankton. Beckmann and

521   Hense (2007) found similar results. Here, we go further to point out an interesting

522   finding that the derivations of the total Chl a are irrespective of the form of the

523   growth limiting function. Since growth functional forms in phytoplankton models are

524   still debated in the literature (Haney, 1996; Ayata et al., 2013), this will be most

525   helpful to estimate the vertical integrated Chl a and primary production.

526   The relationships (in previous sections and in Appendices A and B) we derived can

527   be used to compute missing model parameters (such as maximum growth rate μ_m,

528   loss rate ε, recycling rate α) which are difficult to obtain by on-site observation, if

529   estimates of others are available. For example, Eq. (B4) allows us to obtain an

530   estimate of the sinking velocity of phytoplankton from the measurement of SCM

531   thickness and intensity, the nutrient concentration at water column depth, and the

532   vertical diffusivity below the surface mixed layer.

533   Our analytic solutions can in principle be tested through a comparison with

534   observations: for example, the shape of profiles (the SCML thickness, depth, and

535   intensity), expressed by the characteristic relationships (Eqs. 16-18, 22 and B4), the

536   vertical integral of total subsurface Chl a concentration (Eqs. 21 and B3), the

537   consistency of independent field estimates for sinking velocity, vertical diffusivity,

538   recycling rate and loss rate (Eqs. 21-22 and B3-B4).

We retrieve the three SCM characteristics from Eqs. (16-18, and 22) by combining remote sensing data (annual averaged values of surface light intensity I_0 and light attenuation coefficient K_d) and some parameters from published field and numerical studies (e.g., sinking velocity of phytoplankton w, vertical diffusivity below the surface mixed layer K_{v2}, loss rate ε, maximum growth rate μ_m). Table 2 lists the values of model parameters at three time-series stations in different ocean regions, i.e., the SEATS station, the HOT station, and the BATS (Bermuda Atlantic Time-Series Study) site in the Sargasso Sea, and the corresponding references. The estimated results and the observed values of the SCML thickness, depth and intensity at the three stations are shown in Fig. 2.

The estimated depths and thicknesses of the SCML agree reasonably well with the observations at all three stations. However, the intensities of the SCML are poorly estimated, implying other mechanisms (e.g., wind-driven nutrient pulse) supplying nutrients for the SCML, except upward diffusivity, for phytoplankton growth (Williams et al., 2013). This is the first try to estimate the depth, thickness and intensity of the SCML using parameters from satellite data and field studies. It should be noted that the estimation is sensitive to the used values of these environmental parameters. The values used in estimations above are representative for the averages over a large spatial or temporal scale, but they may not reflect the real values in a specific station. Even though disagreements could be associated with uncertainties from several sources, this type of try would give some idea of how real-world data could be incorporated into the model and thus be applied to the field (Pitarch et al. 2014).

5 Summary

A general Gaussian function is assumed to represent a bell-shape vertical distribution of Chl a in stratified water columns. The function is incorporated into the ecosystem dynamical equations to determine three steady-state SCM characteristics and examine their dependence on environmental parameters such as vertical diffusivity, sinking velocity of phytoplankton, light attenuation coefficient.

The maximum Chl a concentration occurs at or below the location of the maximum growth rates of phytoplankton determined by the vertical mixing time scale and the time taken by a phytoplankton sinking through the length scale.

The depth of the SCML in steady state deepens logarithmically with an increase in surface light intensity, but shoals with increasing light attenuation coefficient, increasing vertical diffusivity below the surface mixed layer, increasing loss rate of phytoplankton, and with decreasing sinking velocity of phytoplankton.

The shape of the SCML (thickness and intensity) is mainly influenced by nutrients supply, but independent of sea surface light intensity. The SCML gets thicker and stronger with a higher vertical diffusivity below the surface mixed layer. The intensity of SCML in steady state weakens as a result of expanding the SCML by a smaller sinking velocity of phytoplankton and a lower light attenuation coefficient.

In regions with a low vertical diffusivity, the SCML depth is inversely proportional to light attenuation coefficient, and is deeper than that in regions dominated by non-sinking phytoplankton. In clear and stable waters with a predominance of small cells, deeper SCMLs can occur with different thicknesses.

Upon potential risk of climate change, it is critical to accurately estimate the global and regional SCML-related primary production. However, the SCM characteristics cannot be detected by remote sensing satellites, which will restrict the application of satellite data in estimating primary production in a large temporal and spatial scale. The Argo float equipped with optical sensor has been developed to measure the distribution of particles and chlorophyll in the world's ocean (Mignot et al., 2014), but the data are still limited. The relationships we derived might help to estimate depth-integrated primary production using available data from satellite observations (incident light and light attenuation coefficient) when appropriate vertical estimates of growth rate and loss rate of phytoplankton, sinking velocity of phytoplankton and vertical diffusivity were adopted based on observations or model results. Again, the solutions could also help to compute environmental parameters that are difficult to obtain from on-site observation.

Appendix A

599 In steady state, the net nutrient flux at any given depth (z) is equals to the net

600 nutrients consumption by phytoplankton, then from steady-state of Eq. (2) we obtain

601 Eq. (A1) below the surface mixed layer:

602
$$\int \left(\mu_m \min\left(f(I), g(N) \right) - \alpha\varepsilon \right) P(z)dz \approx K_{v2} \frac{dN(z)}{dz}\Big|_z \tag{A1}$$

603 If $\mu_m \min(f(I), g(N)) - \varepsilon > 0$, then $\mu_m \min(f(I), g(N)) - \alpha\varepsilon > 0$ for $0 < \alpha \leq 1$, we will

604 have $\dfrac{dN}{dz} > 0$. That is, $N(z)$ will increase with depth below the surface mixed layer.

605 From the properties of the quadratic function in the right hand of Eq. (10), we have

606 $\mu_m \min(f(I), g(N)) - \varepsilon > 0$ on the interval (z_{c1}, z_{c2}). Hence, we have

607 $\mu_m \min(f(I), g(N)) - \alpha\varepsilon > 0$ for $0 < \alpha \leq 1$, then $dN/dz > 0$. In other words, $N(z)$

608 increases with depth on the interval (z_{c1}, z_{c2}).

609 According to Eq. (4), we know that $g(N)$ is a monotonic increasing function on

610 interval (z_{c1}, z_{c2}), and $f(I)$ is a monotonic decreasing function on interval (z_{c1}, z_{c2}).

611 It is well known that the stable SCML occurs in stratified water column only when

612 the growth of phytoplankton in the surface mixed layer is nutrient-limited (Mellard et

613 al., 2011; Ryabov et al., 2010). In other words, the limitation by nutrients $g(N)$ is less

614 than the limitation by light $f(I)$ within the surface mixed layer, i.e., $g(N) < f(I)$ for

615 $0 \leq z \leq z_s$.

616 Because there is only one maximum in the growth rates of phytoplankton which

617 occurs at the depth $z_0 = z_m - \dfrac{w\sigma^2}{2K_{v2}}$, and $z_{c1} < z_0 < z_{c2}$ (Eq. 11), we arrive at

618
$$\min\left(f(I), g(N) \right) = \begin{cases} g(N) & z_{c1} \leq z \leq z_0 \\ f(I) & z_0 \leq z \leq z_{c2} \end{cases} \tag{A2}$$

619 and

620
$$\max\left(\mu_m \min\left(f(I), g(N) \right) \right) = \mu_m f(I)\Big|_{z=z_0}. \tag{A3}$$

621 That is, the maximum growth rate occurs at the depth z_0 where is the transition

622   from nutrients limitation to light limitation, and the growth of phytoplankton is

623   light-limited below the depth z_0 .

Appendix B

The dead phytoplankton is entirely recycled ($\alpha = 1$), and thus the system is closed. In this case, at steady state Eq. (19) reduces to

$$w\frac{dP}{dz} = \frac{d^2}{dz^2}\left(K_v\left(P+N\right)\right) \tag{B1}$$

Integrating this equation twice from the surface to bottom boundary (z_b) gives

$$w\int_0^{z_b} P(z)dz = K_{v1}\left(P+N\right)\Big|_0^{z_s} + K_{v2}\left(P+N\right)\Big|_{z_s+0}^{z_b} \tag{B2}$$

Note that we have known that the SCML occurs only when the growth of phytoplankton within the surface mixed layer is nutrient-limited, then we further assume the surface nutrients value is negligible. Using the assumption of small Chl a at the top and the bottom boundaries of the model domain, we obtain

$$h = \frac{K_{v2}}{w}N\left(z_b\right) \tag{B3}$$

and the intensity of SCML is

$$P_{\max} = \frac{K_{v2}}{\sqrt{2\pi}\sigma w}N\left(z_b\right) \tag{B4}$$

where $N(z_b)$ is the nutrients concentration at depth z_b. Therefore, with $\alpha = 1$, the intensity of SCML is affected by the ambient nutrients concentration below the surface mixed layer. The total Chl a in the water column depends on the sinking velocity of phytoplankton and the diffusivity, but it is independent on the growth rate and loss rate of phytoplankton. Analogous results have been obtained by Liccardo et al. (2013). Beckmann and Hense (2007) also found similar result by introducing an explicit compartment for the detritus in their models.

References:

Anderson, G. C.: Subsurface chlorophyll maximum in the northeast Pacific Ocean, Limnol. Oceanogr., 14, 386-391, 1969.

Ardyna, M., Babin, M., Gosselin, M., Devred, E., Bélanger, S., Matsuoka, A., Tremblay, J. E.: Parameterization of vertical chlorophyll a in the Arctic Ocean: impact of the subsurface chlorophyll maximum on regional, seasonal and annual primary production estimates, Biogeosciences, 10, 4383-4404, doi: 10.5194/bg-10-4383-2013, 2013.

Ayata, S., Lévy, M., Aumont, O., Sciandra, A., Sainte-Marie, J., Tagliabue, A., Bernard, O.: Phytoplankton growth formulation in marine ecosystem models: should we take into account photo-acclimation and variable stoichiometry in oligotrophic areas? J. Marine Syst., 125, 29-40, 2013.

Beckmann, A., Hense, I.: Beneath the surface: Characteristics of oceanic ecosystems under weak mixing conditions-A theoretical investigation, Prog. Oceanogr., 75, 771-796, 2007.

Behrenfeld, M. J., Boss, E. S.: Resurrecting the ecological underpinnings of ocean plankton blooms, Annu. Rev. Mar. Sci., 6, 167-194, 2014.

Bienfang, P. K., Harrison, P. J.: Sinking-rate response of natural assemblages of temperate and subtropical phytoplankton to nutrient depletion, Mar. Biol., 83, 293-300, 1984.

Bowdon, K. F.: Physical oceanography of coastal waters. Limnol. Oceanogr., 30, 449-450, 1985.

Cai Y. M., Ning X. R., Liu C. G.: Synechococcus and Prochlorococcus growth and mortality rates in the northern China Sea: range of variations and correlation with environmental factors. Acta Ecol. Sin. 7, 2237-2246, 2006.

Camacho, A.: On the occurrence and ecological features of deep chlorophyll maxima (DCM) in Spanish stratified lakes, Limnetica, 25, 453-478, 2006.

Chen, C. C., Shiah, F. K., Chung, S. W., Liu, K. K.: Winter phytoplankton blooms in the shallow mixed layer of the South China Sea enhanced by upwelling, J. Marine Syst., 59, 97-110, 2006.

Cianca, A., Godoy, J. M., Martin, J. M., Perez Marrero, J., Rueda, M. J., Llinás, O., Neuer, S.: Interannual variability of chlorophyll and the influence of low‐frequency climate models in the North Atlantic subtropical gyre, Global Biogeochem. Cy., 26, 2012.

Cianca, A., Helmke, P., Mouriño, B., Rueda, M. J., Llinás, O., Neuer, S.: Decadal analysis of hydrography and in situ nutrient budgets in the western and eastern North Atlantic subtropical gyre, J. Geophys. Res., 112, C07025, 1-18, 2007.

Cloern, J. E., Grenz, C., Vidergar-Lucas, L.: An empirical model of the phytoplankton chlorophyll: carbon ratio-the conservation factor between productivity and growth rate, Limnol. Oceanogr., 40, 1313-1321, 1995.

Cullen, J. J., Eppley, R. W.: Chlorophyll maximum layers of the Southern California Bight and possible mechanisms of their formation and maintenance, Oceanol. Acta, 1, 23-32, 1981.

Cullen, J. J.: The deep chlorophyll maximum: comparing vertical profiles of chlorophyll a, Can. J. Fish. Aquat. Sci., 39, 791-803, 1982.

Dekshenieks, M. M., Donaghay, P. L., Sullivan, J. M., Rines, J. E., Osborn, T. R., Twardowski, M. S.: Temporal and spatial occurrence of thin phytoplankton layers in relation to physical processes, Mar. Ecol-Prog. Ser., 223, 61-71, 2001.

Denman, K. L., Gargett, A. E.: Time and space scales of vertical mixing and advection of phytoplankton in the upper ocean, Limnol. Oceanogr., 28, 801-815, 1983.

Fee, E. J.: The vertical and seasonal distribution of chlorophyll in lakes of the Experimental Lakes Area, northwestern Ontario: Implications for primary production estimates. Limnol. Oceanogr., 26, 767-783, 1976.

Fennel, K., Boss, E.: Subsurface maxima of phytoplankton and chlorophyll: Steady-state solutions from a simple model, Limnol. Oceanogr.,, 48, 1521-1534, 2003.

698   Gabric, A. J., Parslow, J.: Effect of physical factors on the vertical distribution of phytoplankton in
699   eutrophic coastal waters, Aust. J. Mar. Fishwater Res., 40, 559-569, 1989.

700   Ghosal, S., Mandre, S.: A simple model illustrating the role of turbulence on phytoplankton blooms, J.
701   Math. Biol., 46, 333-346, 2003.

702   Haney, J. D.: Modeling phytoplankton growth rates, J. Plankton Res., 18, 63-85, 1996.

703   Hanson, C. E., Pesant, S., Waite, A. M., Pattiaratchi, C. B.: Assessing the magnitude and significance
704   of deep chlorophyll maxima of the coastal eastern Indian Ocean, Deep-Sea Res. Pt. II, 54, 884-901,
705   2007.

706   Hense, I., Beckmann, A.: Revisiting subsurface chlorophyll and phytoplankton distributions, Deep-Sea
707   Res. Pt. I, 55, 1193-1199, 2008.

708   Hodges, B. A., Rudnick, D. L.: Simple models of steady deep maxima in chlorophyll and biomass,
709   Deep-Sea Res. Pt. I, 51, 999-1015, 2004.

710   Hood, R. R., Bates, N. R., Capone, D. G., Olson, D. B.: Modeling the effect of nitrogen fixation on
711   carbon and nitrogen fluxes at BATS, Deep-Sea Res. Pt. II, 48, 1609-1648, 2001.

712   Huisman, J., Sommeijer, B.: Maximal sustainable sinking velocity of phytoplankton, Mar. Ecol-Prog.
713   Ser., 244, 39-48, 2002.

714   Huisman, J., Thi, N., Karl, D. M., Sommeijer, B.: Reduced mixing generates oscillations and chaos in
715   the oceanic deep chlorophyll maximum, Nature, 439, 322-325, 2006.

716   Jamart, B. M., Winter, D. F., Banse, K.: Sensitivity analysis of a mathematical model of phytoplankton
717   growth and nutrient distribution in the Pacific Ocean off the northwestern US coast, J. Plankton Res., 1,
718   267-290, 1979.

719   Klausmeier, C. A., Litchman, E.: Algal games: The vertical distribution of phytoplankton in poorly
720   mixed water columns, Limnol. Oceanogr., 8, 1998-2007, 2001.

721   Lee Chen, Y.: Spatial and seasonal variations of nitrate-based new production and primary production
722   in the South China Sea, Deep-Sea Res. Pt. I, 52, 319-340, 2005.

723   Lewis, M. R., Cullen, J. J., Platt, T.: Phytoplankton and thermal structure in the upper ocean:
724   consequences of nonuniformity in chlorophyll profile, J. Geophys. Res., 88, 2565-2570, 1983.

725   Lewis, M. R., Harrison, W. G., Oakey, N. S., Hebert, D., Platt, T.: Vertical nitrate fluxes in the
726   oligotrophic ocean, Science, 234, 870-873, 1986.

727   Liccardo, A., Fierro, A., Iudicone, D., Bouruet-Aubertot, P., Dubroca, L.: Response of the Deep
728   Chlorophyll Maximum to fluctuations in vertical mixing intensity, Prog. Oceanogr., 2013, 33-46, 2013.

729   Liu, H., Chang, J., Tseng, C. M., Wen, L. S., Liu, K. K.: Seasonal variability of picoplankton in the
730   Northern South China Sea at the SEATS station, Deep-Sea Res. Pt. II, 54, 1602-1616, 2007.

731   Lu, Z., Gan, J., Dai, M., Cheung, A.: The influence of coastal upwelling and a river plume on the
732   subsurface chlorophyll maximum over the shelf of the northeastern South China Sea, J. Marine Syst.,
733   82, 35-46, 2010.

734   Mara On, E., Holligan, P. M.: Photosynthetic parameters of phytoplankton from 50° N to 50° S in the
735   Atlantic Ocean, Mar. Ecol.-Prog. Ser., 176, 191-203, 1999.

736   Mellard, J. P., Yoshiyama, K., Litchman, E., Klausmeier, C. A.: The vertical distribution of
737   phytoplankton in stratified water columns, J. Theor. Biol., 269, 16-30, 2011.

738   Mignot, A., Claustre, H., Uitz, J., Poteau, A., D'Ortenzio, F., Xing, X.: Understanding the seasonal
739   dynamics of phytoplankton biomass and the deep chlorophyll maximum in oligotrophic environments:
740   A Bio-Argo float investigation, Global Biogeochem. Cy., 28, 2013G-4781G, 2014.

741   Morel, A.: Optical modeling of the upper ocean in relation to its biogenous matter content (case I
742   waters), J. Geophys. Res., 93, 749-768, 1988.

743   Ono, S., Ennyu, A., Najjar, R. G., Bates, N. R.: Shallow remineralization in the Sargasso Sea estimated
744   from seasonal variations in oxygen, dissolved inorganic carbon and nitrate, Deep-Sea Res. Pt. II, 48,
745   1567-1582, 2001.

746 Oschlies, A.: Model-derived estimates of new production: New results point towards lower values,
747 Deep-Sea Res. Pt. II, 48, 2173-2197, 2001.

748 Pedrós-Alió, C., Calderón-Paz, J. I., Guixa-Boixereu, N., Estrada, M., Gasol, J. M.: Bacterioplankton
749 and phytoplankton biomass and production during summer stratification in the northwestern
750 Mediterranean Sea, Deep-Sea Res. Pt. I, 46, 985-1019, 1999.

751 Pérez, V., Fernández, E., Mara Ón, E., Morán, X., Zubkov, M. V.: Vertical distribution of
752 phytoplankton biomass, production and growth in the Atlantic subtropical gyres, Deep-Sea Res. Pt. I,
753 53, 1616-1634, 2006.

754 Pitarch, J., Odermatt, D., Kawka, M., Wüest, A.: Retrieval of vertical particle concentration profiles by
755 optical remote sensing: a model study, Opt. Express, 22, A947-A959, 2014.

756 Platt, T., Sathyendranath, S., Caverhill, C. M., Lewis, M. R.: Ocean primary production and available
757 light: further algorithms for remote sensing, Deep-Sea Res. Pt. I, 35, 855-879, 1988.

758 Prairie, J. C., Franks, P. J. S., Jaffe, J. S., Doubell, M. J., Yamazaki, H.: Physical and biological
759 controls of vertical gradients in phytoplankton, Limnol. Oceanogr., 1, 75-90, 2011.

760 Raven, J. A., Richardson K.: Photosynthesis in marine environments. In: Topics in Photosynthesis,
761 Elsevier, Edited by N. R. Baker and Long S., 7, 337-399, 1986.

762 Richardson, A. J., Silulwane, N. F., Mitchell-Innes, B. A., Shillington, F. A.: A dynamic quantitative
763 approach for predicting the shape of phytoplankton profiles in the ocean, Prog. Oceanogr., 59, 301-319,
764 2003.

765 Riley, G. A., Stommel, H., Bumpus, D. F.: Quantitative ecology of the plankton of the western North
766 Atlantic, Bulletin Bingham Oceanogra. Collect., 12, 1-69, 1949.

767 Ryabov, A. B., Rudolf, L., Blasius, B.: Vertical distribution and composition of phytoplankton under
768 the influence of an upper mixed layer, J. Theor. Biol., 263, 120-133, 2010.

769 Salihoglu, B., Garçon, V., Oschlies, A., Lomas, M. W.: Influence of nutrient utilization and
770 remineralization stoichiometry on phytoplankton species and carbon export: A modeling study at
771 BATS, Deep-Sea Res. Pt. I, 55, 73-107, 2008.

772 Sharples, J., Moore, C. M., Rippeth, T. P., Holligan, P. M., Hydes, D. J., Fisher, N. R., Simpson, J. H.:
773 Phytoplankton distribution and survival in the thermocline, Limnol. Oceanogr., 46, 486-496, 2001.

774 Siswanto, E., Ishizaka, J., Yokouchi, K.: Estimating chlorophyll-a vertical profiles from satellite data
775 and the implication for primary production in the Kuroshio front of the East China Sea, J. Oceanogr.,
776 61, 575-589, 2005.

777 Sullivan, J. M., Donaghay, P. L., Rines, J. E.: Coastal thin layer dynamics: consequences to biology
778 and optics, Cont. Shelf Res., 30, 50-65, 2010.

779 Sverdrup, H. U.: On conditions for the vernal blooming of phytoplankton, J. Cons. int. Explor. Mer., 18,
780 287-295, 1953.

781 Takahashi, M., Hori, T.: Abundance of picophytoplankton in the subsurface chlorophyll maximum
782 layer in subtropical and tropical waters, Mar. Biol., 79, 177-186, 1984.

783 Tjiputra, J. F., Polzin, D., Winguth, A. M.: Assimilation of seasonal chlorophyll and nutrient data into
784 an adjoint three‐dimensional ocean carbon cycle model: Sensitivity analysis and ecosystem parameter
785 optimization, Global Biogeochem. Cy., 21, GB1001, 1-13, 2007.

786 Varela, R. A., Cruzado, A., Tintoré, J.: A simulation analysis of various biological and physical factors
787 influencing the deep-chlorophyll maximum structure in oligotrophic areas, J. Marine Syst., 5, 143-157,
788 1994.

789 Weston, K., Fernand, L., Mills, D. K., Delahunty, R., Brown, J.: Primary production in the deep
790 chlorophyll maximum of the central North Sea, J. Plankton Res., 27, 909-922, 2005.

791 Williams, C., Sharples, J., Mahaffey, C., Rippeth, T.: Wind‐driven nutrient pulses to the subsurface
792 chlorophyll maximum in seasonally stratified shelf seas, Geophys. Res. Lett., 2013.

793 Wu Y. P., Gao K. S.: Photosynthetic response of surface water phytoplankton assemblages to different

794   wavebands of UV radiation in the South China Sea, Acta Oceanol. Sin., 5, 146-151, 2011.

795   Yoshiyama, K., Mellard, J. P., Litchman, E., Klausmeier, C. A.: Phytoplankton competition for

796   nutrients and light in a stratified water column, Am. Nat., 174, 190-203, 2009.

Growth limitation by light and nutrients

799
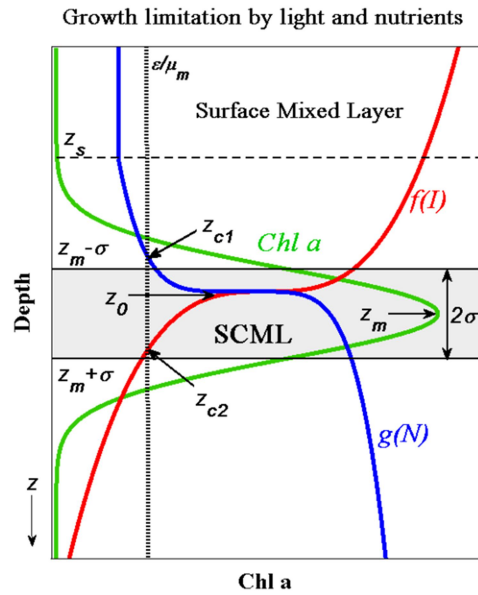
Fig. 1 Schematic picture of Chl a distribution under the limitation by light and nutrient in stratified water columns (green solid line is Chl a concentration as a function of depth; red solid line is the growth limiting term with respect to light, $f(I)$; blue solid line is the growth limiting term with respect to nutrients, $g(N)$; horizontal dashed line represents the depth of surface mixed layer, z_s; horizontal solid lines indicate the locations of the upper- and lower-SCML, $z_m-\sigma$, $z_m+\sigma$, respectively; vertical dotted line is the ratio of loss rate to maximum growth rate, ε/μ_m; z_{c1} and z_{c2} refer to the two compensation depths where $\mu_m g(N)=\varepsilon$ and $\mu_m f(I)=\varepsilon$, respectively; z_0 and z_m indicate the depths of maximum in growth rates and in Chl a concentrations, respectively; double arrow represents the thickness of the SCML, 2σ)

809   Figure 2
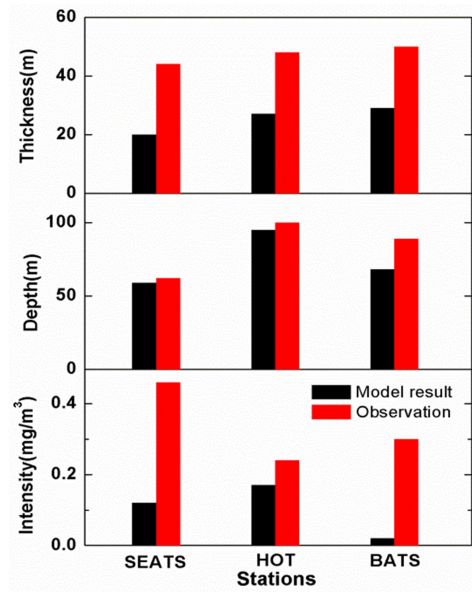
810

811   Fig. 2 Comparisons of the model results and observations (in terms of thickness, depth, and
812   intensity of SCML) at SEATS, HOT, and BATS (black columns represent the model results, red
813   columns are the observations at the three stations which were fitted by Gaussian function using
814   annually averaged data obtained from http://www.odb.ntu.edu.tw/,
815   http://hahana.soest.hawaii.edu/hot/hot-dogs/cextraction.html, and http://bats.bios.edu/,
816   respectively)

817   Table 1 Influences of dynamic model parameters on the steady-state SCML thickness (2σ), depth

818   (z_m), intensity (P_{max}), and the total Chl a in the water column (h).

Model parameters (↑)	2σ	z_m	P_{max}	h
I_0 (Surface light intensity)	-	↑	-	-
K_I (Half-saturation constant of light limited growth)	-	↓	-	-
K_{v2} (Vertical diffusivity below surface mixed layer)	↑	↓	↑	↑
w (Sinking velocity of phytoplankton)	↓	↓	↑	-
K_d (Light attenuation coefficient)	↓	↓	↑	-
ε (Loss rate of phytoplankton)	↓*	↓	/	↓
	↑**	↓	↓	↓
α (Nutrient recycling coefficient)	-	-	↑	↑
$\frac{dN}{dz}\big|_{z=z_b}$ Nutrient gradient at the lower boundary of SCML	-	-	↑	↑
K_N (Half-saturation constant of nutrient limited growth)	-	-	-	-
K_{v1} (Vertical diffusivity in surface mixed layer)	-	-	-	-
μ_{max} (Maximum growth rate of phytoplankton)	/	/	/	/

819   ↑ indicates increase, ↓ indicates decrease, - indicates no effect, / indicates no straightforward

820   result, * indicates a result when $\varepsilon<\mu_{max}/2$, and ** indicates a result when $\varepsilon>\mu_{max}/2$.

821

Table 2 Parameter values at SEATS, HOT, and BATS

Parameters	Units	Values at Stations		
		SEATS	HOT	BATS
I_0	$\mu mol\ photos\ m^{-2}\ s^{-1}$	700 [1, 2]	550 [1, 3]	448 [1, 4]
K_d	m^{-1}	0.052 [1, 5]	0.04 [1, 3]	0.042 [1, 4]
K_{v2}	$m^2\ s^{-1}$	$5*10^{-5}$ [6]	$5*10^{-5}$ [3]	$1*10^{-4}$ [7, 8]
μ_{max}	d^{-1}	1.2 [9, 10]	0.96 [3]	1 [11]
K_I	$\mu mol\ photos\ m^{-2}\ s^{-1}$	40 [12]	20 [3]	20 [3, 12, 13]
ε	d^{-1}	0.5 [9, 10]	0.24 [3]	0.5 [14]
α	-	0.3 [10]	0.5 [3]	0.16 [8]
w	$m\ d^{-1}$	1 [15]	1 [3, 15]	2 [8]
dN/dz at depth of z_b	$mmol\ N\ m^{-4}$	0.1 [16]	0.05 [17, 18]	0.02 [19, 20]
z_b	m	200	200	200

823 Superscripts refer to the references that provide the source for the parameter value and the
824 citations are as follows: [1]http://oceandata.sci.gsfc.nasa.gov/SeaWiFS/Mapped/Annual/9km/;
825 [2]Wu and Gao, 2011; [3]Huisman et al., 2006; [4]Varela et al., 1994; [5]Lee Chen et al., 2005; [6]Lu
826 et al., 2010; [7]Hood et al., 2001; [8]Salihoglu et al., 2008; [9]Cai et al., 2006; [10]Liu et al., 2007;
827 [11]Ayata et al., 2013; [12]Raven and Richardson, 1986; [13]Mara On and Holligan, 1999;
828 [14]Tjiputra et al., 2007; [15]Bienfang and Harrison, 1984; [16]Chen et al., 2006; [17]Fennel and Boss,
829 2003; [18]Hense and Beckmann, 2008; [19]Cianca et al., 2007; [20]Cianca et al., 2012.
830
831
832